Permutation min-entropy: An improved quantifier for unveiling subtle temporal correlations

2015 EPL 109 10005

(http://iopscience.iop.org/0295-5075/109/1/10005)

A Letters Journal Exploring the Frontiers of Physics

January 2015

EPL, **109** (2015) 10005 www.epljournal.org
doi: 10.1209/0295-5075/109/10005

Permutation min-entropy: An improved quantifier for unveiling subtle temporal correlations

Luciano Zunino[1,2(a)], Felipe Olivares[1,3] and Osvaldo A. Rosso[4,5]

[1] *Centro de Investigaciones Ópticas (CONICET La Plata - CIC) - C.C. 3, 1897 Gonnet, Argentina*
[2] *Departamento de Ciencias Básicas, Facultad de Ingeniería, Universidad Nacional de La Plata (UNLP) 1900 La Plata, Argentina*
[3] *Departamento de Física, Facultad de Ciencias Exactas, Universidad Nacional de La Plata (UNLP) 1900 La Plata, Argentina*
[4] *Instituto de Física, Universidade Federal de Alagoas - Maceió, Alagoas, Brazil*
[5] *Instituto Tecnológico de Buenos Aires (ITBA) - Ciudad Autónoma de Buenos Aires, Argentina*

received 31 October 2014; accepted in final form 17 December 2014
published online 20 January 2015

PACS 05.45.Tp – Time series analysis
PACS 89.70.Cf – Entropy and other measures of information
PACS 89.75.-k – Complex systems

Abstract – The aim of this letter is to introduce the *permutation min-entropy* as an improved symbolic tool for identifying the existence of hidden temporal correlations in time series. On the one hand, analytical results obtained for the fractional Brownian motion stochastic model theoretically support this hypothesis. On the other hand, the analysis of several computer-generated and experimentally observed time series illustrate that the proposed symbolic quantifier is a versatile and practical tool for identifying the presence of subtle temporal structures in complex dynamical systems. Comparisons against the results obtained with other tools confirm its usefulness as an alternative and/or complementary measure of temporal correlations.

Introduction. – It is well-known that discriminating the presence of correlations in temporal sequences of measurements or observations, *i.e.* experimental or natural time series, is of vital importance for investigating the dynamics of systems from diverse scientific fields. The identification of time dependencies is essential for classification, modeling, and forecasting purposes. Accordingly, over the last years, much effort has been devoted to developing improved strategies for a more accurate and robust description of the underlying temporal structure [1–5]. Classical methods, like Fourier spectrum and autocorrelation function, require some premises which are seldom satisfied by real data sets [1]. To our knowledge, hitherto, there is not a clear and objective criterion that defines which approach is the most appropriate for each case.

Ordinal methods that consider the temporal ranking information (ordinal or permutation patterns) of the time series can be good alternatives to the traditional methods. They appear to be better suited to cope with usual problems (nonstationarities, nonlinearities, noise distortions) encountered when studying real time series. Within this symbolic scheme, permutation entropy is the most representative and spread descriptor. It is just the celebrated Shannon entropic measure evaluated using the successful recipe introduced by Bandt and Pompe (BP) [6] to extract the probability distribution associated with an input signal. Zhao *et al.* [7] have recently shown that the Rényi permutation entropy, that generalizes the standard (Shannon) permutation entropy, allows for a better characterization of rare and frequent ordinal patterns. Moreover, by analyzing series of autoregressive (AR(1)) processes and the daily closing prices in Shanghai stock market, it is found that the behavior of Rényi permutation entropy as a function of the order q provides a more complete picture of the temporal information of the system dynamics [7].

In this letter, we propose the *permutation min-entropy*, *i.e.* the Rényi permutation entropy in the limit as the order $q \to \infty$, as an improved symbolic quantifier for revealing the presence of subtle temporal correlations in time series. In order to demonstrate this hypothesis, analytical, numerical and experimental results are included.

(a) E-mail: lucianoz@ciop.unlp.edu.ar

Particularly, applications of this quantifier to numerical and experimental data confirm its practical feasibility and utility for several interesting goals, such as detecting structural changes in time series and distinguishing between different sets of physiological —electroencephalogram (EEG) and heart rate variability (HRV)— recordings in both normal and pathological conditions. A multiscale generalization, the *multiscale permutation min-entropy*, has been also proposed for considering the diverse temporal characteristic scales commonly observed in complex system. Furthermore, comparisons against the results obtained by estimating the conventional and weighted permutation entropies suggest that permutation min-entropy can help shed new light on the identification and characterization of the underlying temporal correlations that are present in complex time series. In the following we briefly introduce the permutation min-entropy quantifier, present analytical, numerical and empirical findings, and finally, we end with some concluding remarks.

Permutation min-entropy. – Permutation information-theory–derived quantifier are estimated by implementing the encoding scheme due to BP based on the ordinal relation between the amplitude of neighboring values of a given data sequence. This local ordinal symbolic procedure, that naturally arises from the time series, inherits the causal information that stems from the temporal structure of the system dynamics. Moreover, it avoids amplitude threshold dependencies that affect other more conventional symbolization recipes based on range partitioning [8].

Here, we will illustrate how to create ordinal patterns from the time series data with a simple example. Let us assume that we start with the time series $X = \{3, 2, 5, 8, 9, 6, 1\}$. Two parameters, the embedding dimension $D > 1$ ($D \in \mathbb{N}$, number of symbols that form the ordinal pattern) and the embedding delay τ ($\tau \in \mathbb{N}$, time separation between symbols) are chosen, and next, the time series is partitioned into subsets of length D with delay τ similarly to phase space reconstruction by means of time-delay-embedding. The elements in each new partition (of length D) are replaced by their rank in the subset. For example, if we set $D = 3$ and $\tau = 1$, there are five different three-dimensional vectors associated with X. The first one $(x_0, x_1, x_2) = (3, 2, 5)$ is mapped to the ordinal pattern (102) since $x_1 \leq x_0 \leq x_2$. The second three-dimensional vector is $(x_0, x_1, x_2) = (2, 5, 8)$, and (012) will be its related permutation because $x_0 \leq x_1 \leq x_2$. The procedure continues so on until the last sequence, $(9, 6, 1)$, is mapped to its corresponding motif, (210). Afterward, an ordinal pattern probability distribution, $P = \{p(\pi_i), i = 1, \ldots, D!\}$, can be obtained from the time series by computing the relative frequencies of the $D!$ possible permutations π_i. Continuing with the example: $p(\pi_1) = p(012) = 2/5$, $p(\pi_2) = p(021) = 0$, $p(\pi_3) = p(102) = 1/5$, $p(\pi_4) = p(120) = 1/5$, $p(\pi_5) = p(201) = 0$, and $p(\pi_5) = p(210) = 1/5$. The permutation entropy (PE) is just the Shannon entropy estimated by using this ordinal pattern probability distribution, $S[P] = -\sum_{i=1}^{D!} p(\pi_i) \log(p(\pi_i))$. Coming back to the example, $S[P(X)] = -(2/5)\log(2/5) - 3(1/5)\log(1/5) = 1.3322$. PE quantifies the temporal structural diversity of a time series. Ordinal pattern probability distribution P is obtained once we fix the embedding dimension D and the embedding delay time τ. Taking into account that there are $D!$ potential permutations for a D-dimensional vector, the condition $N \gg D!$, with N the length of the time series, must be satisfied in order to obtain a reliable estimation of P [9]. For practical purposes, BP suggest in their cornerstone paper [6] to estimate the frequency of ordinal patterns with $3 \leq D \leq 7$ and time lag $\tau = 1$ (consecutive points). Nevertheless, other values of $\tau > 1$ (non-consecutive points) might provide additional relevant information as has been recently shown [10,11]. By changing the value of the embedding delay τ different time scales are being considered because τ physically corresponds to multiples of the sampling time of the signal under analysis. For further details about the BP methodology, we strongly recommend refs. [10,12,13], where the construction principle of ordinal patterns and all possible orderings (patterns) for different embedding dimensions are clearly illustrated.

Rényi permutation entropy (RPE), that generalizes the BP permutation entropy, is defined as

$$R_q[P] = \frac{1}{1-q} \log \left(\sum_{i=1}^{D!} p(\pi_i)^q \right), \qquad (1)$$

where the order q ($q \geq 0$ and $q \neq 1$) is a bias parameter: $q < 1$ privileges rare events, while $q > 1$ privileges salient events. The Shannon entropy $S[P]$ is recovered in the limit as $q \to 1$. RPE offers a more flexible tool, allowing for a better characterization of the process under study than just the Shannon permutation entropy counterpart [7]. In the limit as $q \to \infty$, $R_q[P]$ converges to the min-entropy $R_\infty[P]$. Indeed, it can be shown that $R_\infty[P]$ is a function of the highest probability only [14]. Particularly, if the BP encoding is implemented:

$$R_\infty[P] = -\log \left(\max_{i=1,\ldots,D!} p(\pi_i) \right). \qquad (2)$$

We propose this very simple and fast quantifier, hereafter called *permutation min-entropy* (PME), for the purpose of identifying the presence of hidden correlational structures in complex time series. Of course, PME retains all the advantages of the conventional PE, namely, i) simplicity, ii) low computational cost, iii) noise robustness, and iv) invariance with respect to nonlinear monotonous transformations [6]. These properties are highly appreciated for the analysis of experimental data. Moreover, this entropic measure is applicable to noisy real time series from all class of systems, deterministic and stochastic, without the need to require any assumption about the generating process [15]. Henceforth, normalized quantifiers are estimated

taking into account that the maximum value for RPE, obtained from an equiprobable ordinal pattern probability distribution, is equal to $\log(D!)$ independently of q.

Fractional Brownian motion: analytical and numerical analysis. – Fractional Brownian motion (fBm) is a widely accepted theoretical framework to model fractal phenomena which have power-law decaying power spectral density $1/f^{\alpha}$ with $1 < \alpha < 3$ [16]. This non-stationary stochastic process is Gaussian, self-similar and it has stationary increments (fractional Gaussian noise (fGn)). Its intrinsic long-range dependences are quantified through the Hurst exponent $H \in (0, 1)$ with $\alpha = 2H + 1$. When $H > 1/2$, consecutive increments tend to have the same sign so that these processes are *persistent* ([17], Chapt. 9). For $H < 1/2$, on the other hand, consecutive increments are more likely to have opposite signs, and it is said that the processes are *anti-persistent* ([17], Chapt. 9). The standard memoryless Brownian motion (random walk) is recovered for $H = 1/2$. Much effort has been dedicated to the characterization of this family of fractal stochastic processes [18–22].

Bandt and Shiha have previously found theoretical expressions for the probabilities of the ordinal patterns of fBm for embedding dimensions $D = 3$ and $D = 4$ [2]. Extension of these results for larger embedding dimensions is not trivial. Since these processes are self-similar, the ordinal pattern relative frequencies result independent of the embedding delay (time scale) τ. Using these analytical findings, in fig. 1, we have plotted RPE for different orders q and $D = 4$ as a function of the Hurst exponent H. As can be seen, the sensitivity of RPE to characterize different temporal correlations increases with q because the difference between values of the quantifier for two similar Hurst exponents is amplified. Indeed, for large values of q, its performance as a correlation descriptor is much better than that of PE (plotted in dashed line in fig. 1).

Going in depth over this finding, numerical and analytical results for the PME, *i.e.* $\lim_{q\to\infty}\mathrm{RPE}$, of fBm processes are illustrated in fig. 2. Mean and standard deviation of the estimated PME values (eq. (2) with $3 \leq D \leq 6$ and $\tau = 1$) for 1000 independent fBm realizations of length $N = 10000$ data points with Hurst exponent $H \in \{0.05, 0.1, \ldots, 0.95\}$ are shown. Artificial fBm time series were generated by implementing two different algorithms. On the one hand, the method of Wood and Chan [23] was adopted for numerical simulations of signals with $H \leq 0.5$ and, on the other hand, persistent time series were generated via the function *wfbm* of MATLAB, that follows the algorithm proposed by Abry and Sellan [24]. Taking into account that artificial series generators are obviously not exact, this choice allows for an improved agreement between numerical and theoretical results.

According to the findings obtained, it can be concluded that, within the family of permutation Rényi entropies, PME is the optimal one for the purpose of discriminating between fBm with different Hurst exponents. It exhibits the largest range of estimated values allowing for an enhanced distinction of the underlying correlations of the processes under study. Moreover, since a roughly linear dependence holds between PME and H, an improved characterization of the fBm processes is achieved with this particular information-theory–derived quantifier.

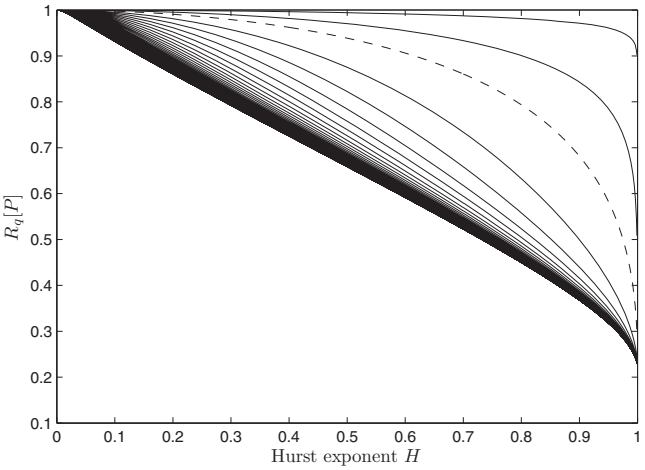

Fig. 1: Theoretical RPE as a function of the Hurst exponent H for fBm processes. Bias parameter q ($q \in \{0.1, 0.5, 2, 3, \ldots, 99, 100\}$) is increasing from top to bottom. PE is also plotted (dashed line). Analytical curves for embedding dimension $D = 4$ are shown. A similar behavior is observed for $D = 3$.

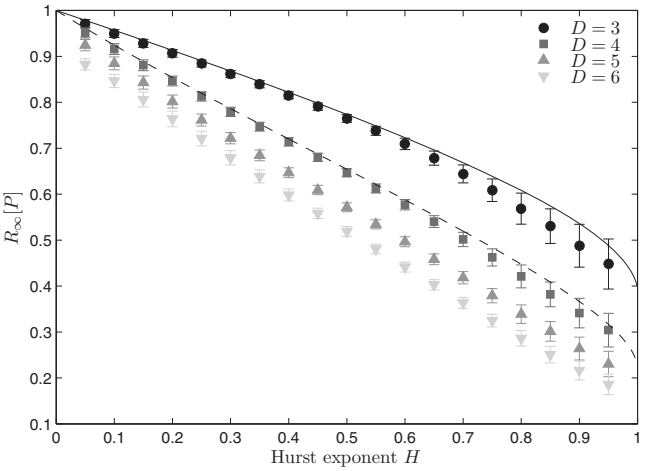

Fig. 2: PME as a function of the Hurst exponent H for fBm processes. Numerical results for different embedding dimensions (D from 3 to 6) are plotted. Mean and standard deviation from 1000 independent fBm simulations of length $N = 10000$ data points are depicted ($H \in \{0.05, 0.1, \ldots, 0.95\}$). Analytical curves for $D = 3$ (continuous line) and $D = 4$ (dashed line) are also included for comparison purposes.

Numerical and experimental applications. – In a first controlled example we consider the identification of underlying structural changes from time series. For this purpose we generate a time series that results from the combination of other two with similar but not

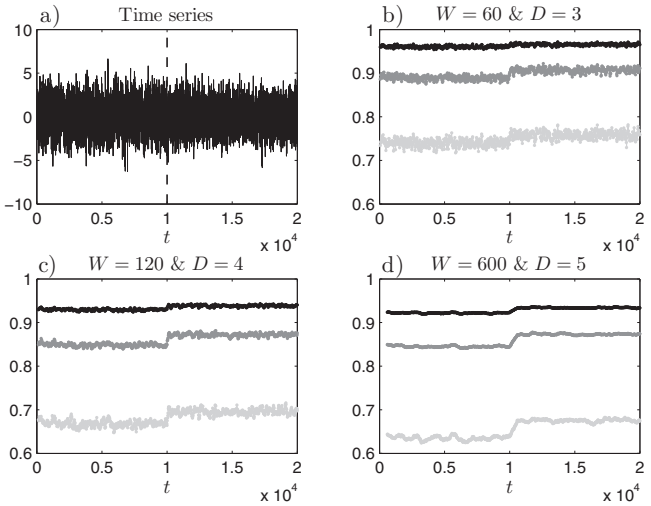

Fig. 3: Time-dependent PME (light gray), PE (black) and WPE (dark gray) applied to identify the transition between two slightly different dynamical regimes. (a) Representative time series obtained by merging two similar AR(1) processes with the dynamical change located at the middle (dashed line). (b) Estimated values for the three permutation symbolic quantifiers by implementing a dynamical analysis with sliding windows of size $W = 60$ and $D = 3$. (c) The same as (b) but with $W = 120$ and $D = 4$. (d) The same as (b) but with $W = 600$ and $D = 5$. In the three cases time windows were slided by 20 samples and the embedding delay was set equal to 1. Average value of the estimated quantifiers over 100 independent realizations are plotted.

identical characteristics. Following the analysis proposed by Cánovas *et al.* [25], we have simulated two AR(1) processes — $x_t = ax_{t-1} + \epsilon_t$ where ϵ_t are pseudorandom values from the standard normal distribution — of length $N = 10000$ data points with two quite close values of the parameter a ($a = 0.8$ and $a = 0.7$). The time series for testing, of length $N = 20000$, is obtained by merging these two similar AR(1) simulations, *i.e.* the first half of the new time series corresponds with the AR(1) process simulated for $a = 0.8$ and the second half with the AR(1) process generated for $a = 0.7$. We are trying to test how successful results PME for detecting the transition between different dynamical regimes artificially introduced at the middle of the time series. A dynamical analysis was implemented by estimating this quantifier through sliding time windows that move along the original signal. Results obtained for different window sizes W and embedding dimensions D are depicted in fig. 3. In all cases consecutive sliding time windows were displaced by 20 samples and results were averaged over 100 independent realizations. PE and weighted permutation entropy (WPE) were also estimated for performance comparison. WPE was introduced in ref. [26] as a variation of the standard permutation entropy in which amplitude information is incorporated in the algorithm for estimating the ordinal pattern relative frequencies. Improvements in the analysis of data with spiky features or having abrupt changes in magnitude have been confirmed by using this weighted scheme [26]. From figs. 3(b)–(d) it can be concluded that PME allows for a clear discrimination between the two similar dynamics. Its sensitivity to detect transitions in the underlying dynamics is notably improved compared with the PE, and it attains a similar performance than the WPE. It is worth remarking here that WPE has been shown particularly useful for detecting dynamical changes [26].

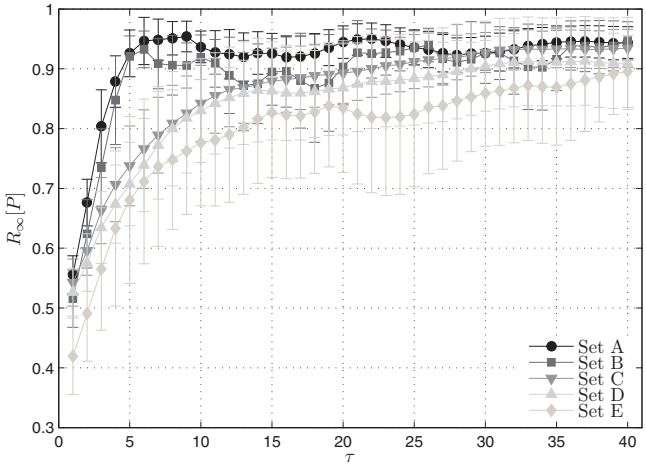

Fig. 4: Multiscale PME with $D = 3$ for the EEG database. Mean and standard deviation of the estimated values for PME over the 100 data segments associated with each EEG group are plotted as a function of the embedding delay τ. Similar results are obtained for other embedding dimensions ($4 \leq D \leq 6$).

In order to illustrate the performance of the proposed quantifier in real contexts we next describe how it can be used to discriminate different sets of normal and pathological physiological data. More precisely, as a first practical application, we analyze, via PME, five different sets of EEGs for healthy and epileptic patients that were previously analyzed by Andrzejak *et al.* [27] (available at `http://www.meb.unibonn.de/epileptologie/science/physik/eegdata.html`). The data consist of 100 data segments, whose length is 4097 data points with a sampling frequency of 173.61 Hz, of brain activity for different groups and recording regions: surface EEG recordings from five healthy volunteers in an awake state with eyes open (Set A) and closed (Set B), intracranial EEG recordings from five epilepsy patients during the seizure free interval from outside (Set C) and from within (Set D) the seizure generating area, and intracranial EEG recordings of epileptic seizures (Set E). Details about the recording technique of these EEG data can be found in the original paper. Since the discrimination between the different groups will depend on the time scale used for the analysis and, *a priori*, the optimal time scale for such a purpose is unknown, we implement a multiscale PME strategy by analyzing the behavior of PME as a function of the embedding delay τ for a chosen embedding dimension. Results obtained from this multiscale analysis are represented in fig. 4. More precisely, mean and

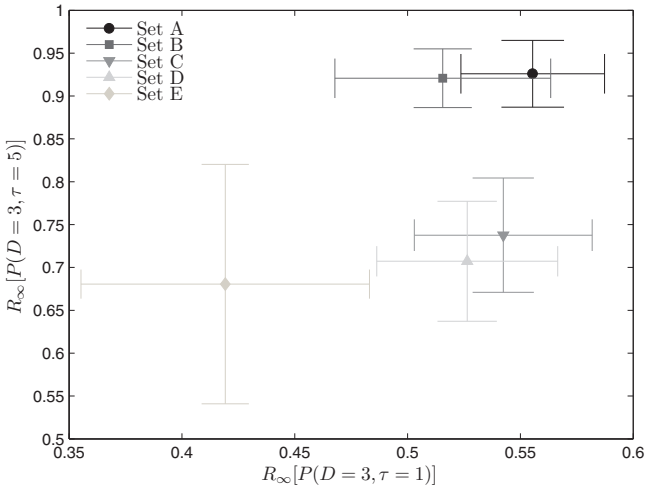

Fig. 5: PME estimated from the EEG database with $D = 3$ and $\tau = 5$ is plotted as a function of the same quantifier but for $D = 3$ and $\tau = 1$. Mean and standard deviation of the estimated values over the 100 data segments associated with each EEG group are represented. This bidimensional scheme is able to discriminate between the different EEG data sets.

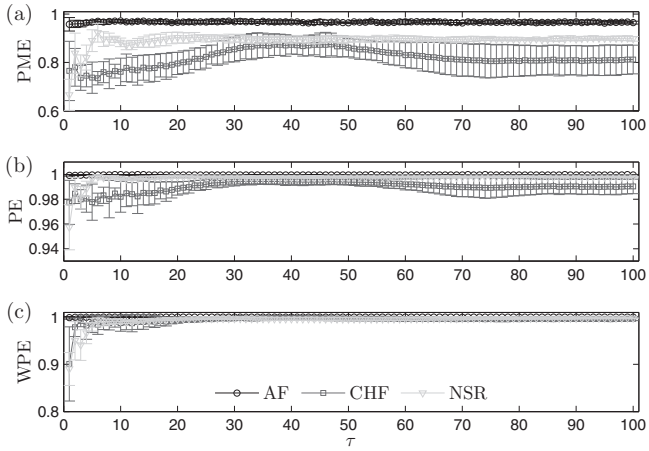

Fig. 6: (a) Multiscale PME with $D = 3$ for the HRV database. Mean and standard deviation of PME as a function of the embedding delay τ for the three groups (AF, CHF and NSR). (b) The same for PE. (c) The same for WPE. Results obtained for higher embedding dimensions ($4 \leq D \leq 6$) are similar.

standard deviation of the estimated PME with $D = 3$ over the 100 realizations of each group are plotted as a function of τ. Similar results are obtained by using other embedding dimension ($4 \leq D \leq 6$).

From this multiscale analysis we conclude that an improved distinction between the different groups is possible through a bidimensional scheme in which PME estimated for two different time delays ($\tau = 1$ and $\tau = 5$) are plotted together. These two scales of observation are the optimal ones to achieve an efficient group differentiation according to the p-values of a standard two-sample t-test. A minimal p-value is obtained for embedding delay $\tau = 5$ for distinguishing between the different pairs of non-epileptic and seizure free data with the PME estimated values. Equivalently, the p-value as a function of the time scale has a minimum for $\tau = 1$ when comparing the PME related values of the two pathological groups (no seizure vs seizure). As can be seen in fig. 5, different planar locations are obtained for the healthy (Sets A and B) and unhealthy groups (Sets C, D and E). Furthermore, data sets from patients during the seizure free interval (Sets C and D) and those corresponding to epileptic seizures (Set E) are also separated. We have found that EEG segments from healthy subjects from both sets (eyes open and closed) have larger estimated PME values than those associated with the other groups for $\tau = 5$. Likewise, PME estimated with the original sampling frequency, *i.e.* $\tau = 1$, results smaller for EEGs of patients during the epileptic seizure than those obtained during seizure free intervals. Use of pairs of features for biosignal classification has been proposed by Parlitz *et al.* [10]. We have confirmed that equivalent bidimensional procedures for PE and WPE are not as efficient as group discriminators. Moreover, our findings are consistent with those derived from other approaches much more complicated, both computationally and conceptually [28,29].

As a second real application, we have implemented the multiscale PME, *i.e.* the PME as a function of the embedding delay τ, for distinguishing a collection of 15 heart beat interval (RR-interval) time series of which five were obtained from healthy persons in normal sinus rhythm (NSR), five from congestive heart failure (CHF) patients, and five from subjects suffering from atrial fibrillation (AF). These time series, made freely available by PhysioNet (`http://www.physionet.org/challenge/chaos/`), are about 24 hours long (roughly 100000 intervals). Original records, without applying any filter, were considered. Mean and standard deviation values of PME estimated for $D = 3$ and $1 \leq \tau \leq 100$ are shown in fig. 6(a) for the three groups. A clear discrimination between them is reached with the proposed symbolic quantifier for two different ranges of temporal scales: when $\tau \in [5, 25]$ and for embedding delays larger than 70. In fig. 6(b) and fig. 6(c) similar analysis are illustrated for the PE and WPE, respectively. It can be easily concluded the higher discriminative power of PME.

Results obtained in both physiological analysis support that the multiscale PME can be a promising potential feature for biosignal classification. It is able to magnify the temporal correlation differences between two or more systems at several scales of observation simultaneously.

Conclusions. – In this letter, we introduce a very simple and fast symbolic quantifier, namely the permutation min-entropy, to deal with the identification of intricate temporal structures from time series data. This is an essential issue for a comprehensive understanding and modeling of the intrinsic dynamics of the investigated system from which a time series has been measured. We

report analytical, numerical and empirical evidences that allows us to confirm the reliability and robustness of the permutation min-entropy for detecting the presence of subtle temporal correlations. As the EEG and HRV examples confirm, if necessary, a multiscale generalization of this quantifier can be easily implemented to take into account the multiple time scales usually involved in complex systems. We conclude by encouraging researchers to use this quantifier in their fields of interest for testing its advantages as a discriminator of the temporal structure present in time series. Interested readers are welcome to contact the authors for an implemented code in MATLAB.

* * *

LZ and FO acknowledge Consejo Nacional de Investigaciones Científicas y Técnicas (CONICET), Argentina and Universidad Nacional de La Plata, Argentina for their support. OAR acknowledges support from CONICET, Argentina, and FAPEAL, Brazil.

REFERENCES

[1] Bandt C., *Ecol. Model.*, **182** (2005) 229.
[2] Bandt C. and Shiha F., *J. Time Ser. Anal.*, **28** (2007) 646.
[3] Rubido N., Tiana-Alsina J., Torrent M. C., Garcia-Ojalvo J. and Masoller C., *Phys. Rev. E*, **84** (2011) 026202.
[4] Grech D. and Miśkiewicz J., *EPL*, **97** (2012) 30005.
[5] Aragoneses A., Perrone S., Sorrentino T., Torrent M. C. and Masoller C., *Sci. Rep.*, **4** (2014) 4696.
[6] Bandt C. and Pompe B., *Phys. Rev. Lett.*, **88** (2002) 174102.
[7] Zhao X., Shang P. and Huang J., *EPL*, **102** (2013) 40005.
[8] Bollt E. M., Stanford T., Lai Y.-C. and Życzkowski K., *Phys. Rev. Lett.*, **85** (2000) 3524.
[9] Staniek M. and Lehnertz K., *Int. J. Bifurcat. Chaos*, **17** (2007) 3729.
[10] Parlitz U., Berg S., Luther S., Schirdewan A., Kurths J. and Wessel N., *Comput. Biol. Med.*, **42** (2012) 319.
[11] Zunino L., Soriano M. C. and Rosso O. A., *Phys. Rev. E*, **86** (2012) 046210.
[12] Zanin M., Zunino L., Rosso O. A. and Papo D., *Entropy*, **14** (2012) 1553.
[13] Riedl M., Müller A. and Wessel N., *Eur. Phys. J. ST*, **222** (2013) 249.
[14] Grigorescu S. and Petkov N., in *Proceedings of the International Conference on Image Processing (ICIP)*, Vol. **1** (IEEE) 2003, p. 241.
[15] Garland J., James R. and Bradley E., *Phys. Rev. E*, **90** (2014) 052910.
[16] Mandelbrot B. B. and Van Ness J. W., *SIAM Rev.*, **10** (1968) 422.
[17] Feder J., *Fractals* (Plenun Press, New York) 1988.
[18] Gao J. B., Cao Y. and Lee J.-M., *Phys. Lett. A*, **314** (2003) 392.
[19] Zunino L., Pérez D. G., Martín M. T., Garavaglia M., Plastino A. and Rosso O. A., *Phys. Lett. A*, **372** (2008) 4768.
[20] Zunino L., Pérez D. G., Kowalski A., Martín M. T., Garavaglia M., Plastino A. and Rosso O. A., *Physica A*, **387** (2008) 6057.
[21] Lacasa L., Luque B., Luque J. and Nuño J. C., *EPL*, **86** (2009) 30001.
[22] Makarava N., Benmehdi S. and Holschneider M., *Phys. Rev. E*, **84** (2011) 021109.
[23] Coeurjolly J.-F., *J. Stat. Softw.*, **5** (2000) 1.
[24] Abry P. and Sellan F., *Appl. Comput. Harmon. Anal.*, **3** (1996) 377.
[25] Cánovas J. S., Guillamón A. and Ruiz M. C., *Fluct. Noise Lett.*, **10** (2011) 13.
[26] Fadlallah B., Chen B., Keil A. and Príncipe J., *Phys. Rev. E*, **87** (2013) 022911.
[27] Andrzejak R. G., Lehnertz K., Mormann F., Rieke C., David P. and Elger C. E., *Phys. Rev. E*, **64** (2001) 061907.
[28] Adeli H., Ghosh-Dastidar S. and Dadmehr N., *IEEE Trans. Biomed. Eng.*, **54** (2007) 205.
[29] Gao J., Hu J. and Tung W. W., *PLoS ONE*, **6** (2011) e24331.